High-precision mass measurement of ²⁴Si and a refined determination of the rp process at the A = 22 waiting point

D. Puentes, 1,2,* Z. Meisel, 3,4 G. Bollen, 1,5 A. Hamaker, 1,2 C. Langer, E. Leistenschneider, 2 C. Nicoloff, 1,2 W.-J. Ong, ^{7,4} M. Redshaw, ^{2,8} R. Ringle ⁶, ² C. S. Sumithrarachchi, ² J. Surbrook ⁶, ^{1,2} A. A. Valverde ⁶, ⁹ and I. T. Yandow ⁶, ^{1,2} ¹Department of Physics and Astronomy, Michigan State University, East Lansing, Michigan 48824, USA ²National Superconducting Cyclotron Laboratory, East Lansing, Michigan 48824, USA ³Institute of Nuclear & Particle Physics, Department of Physics and Astronomy, Ohio University, Athens, Ohio 45701, USA 4 Joint Institute for Nuclear Astrophysics – Center for the Evolution of the Elements, Michigan State University, East Lansing, Michigan 48824, USA ⁵Facility for Rare Isotope Beams, East Lansing, Michigan 48824, USA ⁶University of Applied Sciences Aachen, 52066 Aachen, Germany ⁷Nuclear and Chemical Sciences Division, Lawrence Livermore National Laboratory, Livermore, California 94550, USA ⁸Department of Physics, Central Michigan University, Mount Pleasant, Michigan 48859, USA ⁹Department of Physics and Astronomy, University of Manitoba, Winnipeg, Manitoba, Canada R3T 2N2



(Received 7 June 2021; revised 26 August 2021; accepted 22 June 2022; published 5 July 2022)

We report a high-precision mass measurement of ²⁴Si, performed with the Low Energy Beam and Ion Trap (LEBIT) facility at the National Superconducting Cyclotron Laboratory. The atomic mass excess, 10753.8(37) keV, is a factor of 5 more precise than previous results. This substantially reduces the uncertainty of the 23 Al $(p, \gamma)^{24}$ Si reaction rate, which is a key part of the rapid proton capture (rp) process powering type I x-ray bursts. The updated rate constrains the onset temperature of the (α, p) process at the ²²Mg waiting point to a precision of 9%.

DOI: 10.1103/PhysRevC.106.L012801

Type I x-ray bursts occur at astrophysical sites consisting of a binary star system where a neutron star accretes H/He-rich matter from a companion star, leading to nuclear burning on the neutron star surface [1,2]. As the temperature increases, the hot CNO cycle proceeds until the triple- α process is initiated with an ensuing thermonuclear runaway. The thermonuclear runaway explosion consists of multiple competing reaction sequences including the rapid proton (rp)[3] and (α, p) [4] processes. The rate at which the runaway occurs as well as the reaction sequence competition depends on factors such as accretion rate and fuel composition. The only observable from these explosions, however, is the x-ray burst light curve, which can be recorded with telescopes like the Neutron Star Interior Composition Explorer (NICER) [5].

In addition to the astrophysical conditions, the main determinant of the shape of the light curve is the nuclear physics involved [6]. The nuclear physics input consists of the fast (p, γ) , (α, γ) , and (α, p) reaction rates and slow β^+ decays. Single-zone [7] and multizone [8,9] x-ray burst models have been used to understand the impact of the uncertainties derived from these nuclear physics inputs [10,11]. Through these analyses, it was shown that only a few reactions play a large role in the uncertainties of the simulated light curves [10]. The dramatic variations in the simulated light curve due to these

reaction rate uncertainties can make it difficult to extract astrophysical parameters from comparisons with observed bursting

One of those influential reactions is the 23 Al $(p, \gamma)^{24}$ Si reaction. Variations within the uncertainty of this reaction rate lead to significant shifts in the simulated x-ray light curve. The importance of this reaction stems from its direct connection to the 22 Mg waiting point along the rp process [12]. The Qvalue for $^{22}\text{Mg}(p, \gamma)$ (0.141 MeV) [13] is small enough to establish a (γ, p) - (p, γ) equilibrium [14], which makes it difficult for the rp process to proceed in this mass region. There is evidence [14] that the ²²Mg waiting point can be bypassed via the 22 Mg(α , p) reaction. However, it is also possible for the 23 Al (p, γ) reaction to undergo resonant capture to only a few low-lying states in ²⁴Si when certain conditions are assumed for x-ray bursts. This network competition in the reaction flow has been investigated in previous experiments, providing constraints on when $^{22}Mg(\alpha, p)$ becomes significant during x-ray burst events [15]. However, uncertainties in the 23 Al (p, γ) reaction need to be resolved in order to confirm the flow of the rp process at this waiting point. A recent experiment measured γ rays from ²³Al(d, n) [16] to identify unbound states in ²⁴Si, making the uncertainty in the mass of ²⁴Si (19 keV [13]) the dominant source of uncertainty for the 23 Al (p, γ) reaction rate. A high-precision mass measurement of 24 Si would constrain the rp process in this mass region by precisely quantifying the bypass of the ²²Mg waiting point.

^{*}puentes@frib.msu.edu

In this Letter, we present a new high-precision mass measurement of ²⁴Si using Penning trap mass spectrometry.

A beam of ²⁴Si was produced at the National Superconducting Cyclotron Laboratory [17] via projectile fragmentation of a ²⁸Si¹⁴⁺ beam, at an energy of 160 A MeV, with a 1530 mg/cm² thin beryllium foil target. The resulting cocktail beam was purified using the A1900 fragment separator [17]. Afterwards, the beam was sent through a momentum compression beamline, passing through aluminum degraders and an Al wedge to degrade the beam energy before entering the gas stopper [18]. Interactions between the ²⁴Si ions and the helium gas in the stopper slowed the rare isotope ions, which were then extracted using a combination of direct current and radio frequency (RF) fields. After extraction from the gas cell, the rare isotope ions were injected into a radio frequency quadrupole (RFQ), accelerated to an energy of 30 keV and purified with a magnetic dipole mass separator based on their mass-to-charge ratio (A/Q). Following the beam stopping facility, ²⁴Si was delivered as a molecular ion, [²⁴SiO₂H]⁺, at A = 57. The beam was then transported to the Low Energy Beam and Ion Trap (LEBIT) [19] facility where the mass measurements were performed.

The first component of the LEBIT facility is a beam cooler and buncher [20]. The ions were cooled, collected, and ejected as a pulsed beam. The pulsed ion beam was subsequently injected into the 9.4-T Penning trap mass spectrometer [21] and directed off-axis relative to the trap center using Lorentz steerers [22], capturing the ions in an initial magnetron orbit. During trapping, contaminants were purged using a sum of dipole RF excitations at the identified contaminants' reduced cyclotron frequencies and a broadband stored wave-form inverse Fourier transform (SWIFT) excitation [23,24] to remove contaminant ions. The major contaminants identified during the experiment were $[C_3H_2F]^+$, $[C_2HS]^+$, and $[C_3H_5O]^+$. The time-of-flight ion cyclotron resonance technique was then used to measure the mass of the ion of interest. In this method, a quadrupole excitation is performed for a range of frequencies near the cyclotron frequency, $v_c = qB/2\pi m$, of the ion of interest [25,26]. As the RF excitation v_{RF} approaches v_c , the magnetron motion is converted to reduced cyclotron motion. The conversion is maximized when $\nu_{RF} \approx \nu_c$. Following the excitation, the ions are ejected from the trap to a microchannel plate detector, where the time of flight is recorded. During the conversion, the ions gain energy, which is observed as a minimum in the TOF response curve. The theoretical line shape can be fit to the data to extract v_c [26].

Another excitation scheme, known as a Ramsey excitation [27], was also performed in this experiment. This generates a TOF pattern visible in Fig. 1 and described by Ref. [27], which allows superior precision to the simple RF excitation scheme for the same ion trapping times. Eighteen measurements of [24SiO₂H]⁺ were performed, consisting of 6 normal quadrupole excitation measurements and 12 Ramsey excitation measurements. The normal quadrupole excitation measurements were performed with 50- and 75-ms excitations. The Ramsey measurements were performed with 25-, 50-, 75-, 100-, and 150-ms excitations.

Cyclotron frequency measurements of [24SiO₂H]⁺ were bracketed between two reference measurements

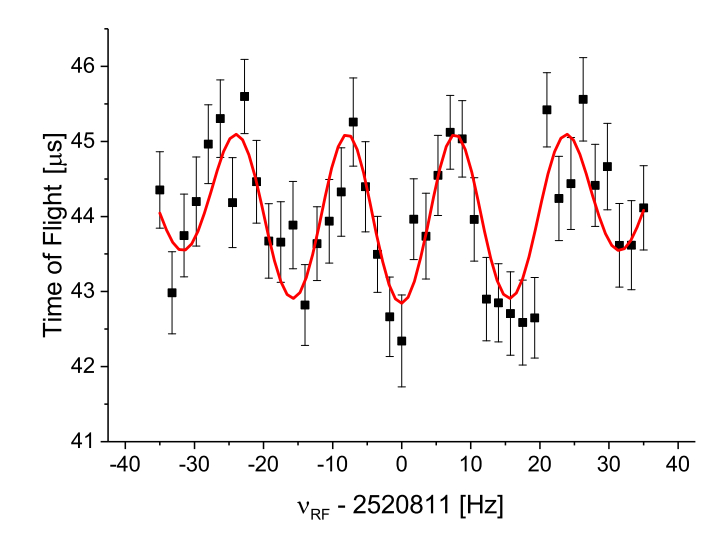


FIG. 1. An example of a 75-ms $[^{24}\text{SiO}_2\text{H}]^+$ time-of-flight Ramsey cyclotron resonance curve from which ν_c was determined. The line shape is described in Ref. [27].

of [12C₃H₂F]⁺ to track variations in the magnetic field strength. The weighted average of the ratio for $v_c([^{24}SiO_2H]^+)/v_c([^{12}C_3H_2F]^+)$ was determined to be $\bar{R} = 1.000\,085\,151(71)$ with an associated Birge ratio [28] of 1.03. Most systematic uncertainties in \bar{R} scale linearly with the mass difference between the ion of interest and the reference ion [25]. This mass-dependent shift has been measured to be $\Delta \bar{R} = 2 \times 10^{-10} / \text{u}$ [29], which is negligible for isobaric species. Other systematic uncertainties include relativistic effects, ion-ion interactions, and nonlinear magnetic field fluctuations. Relativistic effects are negligible compared to the statistical uncertainty [30]. Ion-ion interactions were limited by excluding shots with more than five ions. The nonlinear fluctuations in the magnetic field are on the order of $\Delta \bar{R} = 10^{-9}/h$ [31]. The longest single measurement was 2.5 h, making these fluctuations negligible as well. As a result, the uncertainty of our averaged frequency measurement is statistical.

The mass excess of 24 Si was extracted directly from \bar{R} and was determined to be 10 753.8(37) keV. Our mass is in good agreement with the AME2020 value [10 745(19) keV] and a factor of 5 more precise. The AME2020 value is primarily based on a 1980 pion double-charge exchange reaction measurement [32]. With our measurement, a new proton separation energy for 24 Si was calculated to be 3283.2(37) keV.

With a precisely known Q value, the flow following the 22 Mg waiting point in the rp process is strictly constrained based on nuclear physics information. Figure 2 displays the impact of the new Q value on the uncertainty of the 23 Al(p, γ) reaction rate. Also shown in Fig. 2 are the 22 Mg(p, γ) reaction rate, which is represented by the black band, based on information from Ref. [33], and the reaction rate experimentally determined for the 22 Mg(α , p) reaction represented by the blue band from Ref. [15]. We estimate the 22 Mg(α , p) reaction rate uncertainty to be $\pm 80\%$ based on the uncertainty for the lowest-energy cross-section measurement from Ref. [15].

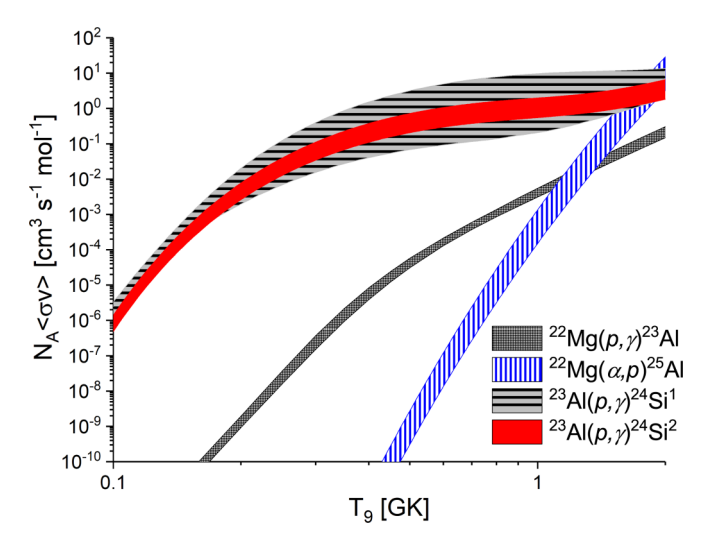


FIG. 2. The reaction rates for 23 Al (p, γ) (Wolf *et al.* [16], denoted by the superscript 1, and this work, denoted by the superscript 2), 22 Mg (p, γ) (Iliadis *et al.* [33]), and 22 Mg (α, p) (Randhawa *et al.* [15]) from 0.1 to 2 GK. Our calculations show a dramatic reduction in the 1- σ reaction rate uncertainty for 23 Al (p, γ) as a result of our new mass measurement and the corresponding resonance energies.

The 23 Al (p, γ) reaction rate was calculated using the narrow resonance approximation [34]. The information that contributed to this calculation can be found in Table I, based on experimental information [16] and, for higher-lying states, on calculations with NUSHELLX@MSU [35] that were included

TABLE I. Resonance levels used in the narrow-resonance approximation for the reaction rate calculation. Experimental information is taken from Ref. [16]. Other levels were calculated with the NUSHELL@MSU package with their corresponding spectroscopic factors, radiative widths, and proton widths [35], as denoted by *. Excitation energies from NUSHELLX@MSU calculations were defined with uncertainties of 150 keV [38]. The reaction rate was calculated with a Monte Carlo program to determine a robust rate uncertainty. A complete description of the reaction rate calculation can be found in the text.

E_x (MeV)	J	l	C^2S	Γ_{γ} (eV)	Γ_p (eV)
3.449(5)	2	0	0.7(4)	1.9×10^{-2}	1.0×10^{-4}
,		2	0.002(1)		
		2	0.3(2)		
3.471(6)	0	2	0.8(4)	1.6×10^{-3}	6.2×10^{-5}
4.256(150)*	3	0	0.59	1.3×10^{-2}	9.0×10^{3}
		2	0.17		
5.353(150)*	3	0	0.0012	2.8×10^{-2}	3.6×10^{3}
		2	0.11		
5.504(150)*	2	0	0.044	2.2×10^{-1}	2.8×10^{4}
		2	0.068		
5.564(150)*	4	2	0.048	2.2×10^{-2}	2.2×10^{3}
6.004(150)*	4	2	0.28	6.5×10^{-3}	2.8×10^{4}
6.056(150)*	0	2	0.053	3.4×10^{-3}	5.6×10^{3}
6.072(150)*	2	0	0.012	5.0×10^{-2}	2.4×10^{4}
		2	0.093		

in the reaction rate calculation of Ref. [16]. Based on a previous measurement of longitudinal momentum distributions of 24 Si states [36], we assigned the 3471 state with J=0 and used the information from Ref. [16].

The reaction rate properties varied using a Monte Carlo random-sampling approach. The excitation energies in the unbound states of 24 Si and the Q value for the 23 Al (p, γ) reaction were varied, assuming a normal distribution. The impact of the proton penetration factor was also included in the reaction rate calculation [37]. The excitation energies derived from NUSHELLX@MSU calculations were defined with uncertainties of 150 keV [38]. The radiative widths and spectroscopic factors were varied with a log-normal distribution [39]. All radiative partial widths assumed a factor uncertainty of 2 [40]. The same factor uncertainty was used for all theoretical spectroscopic factors. Experimental spectroscopic factors and uncertainties were varied using relations found in Ref. [39]. The proton partial widths were scaled, based on the impact of the spectroscopic factor variation.

For the direct capture component of the reaction rate calculation, the spectroscopic factors for each astrophysical S factor reported in Ref. [41] were varied with a log-normal distribution as well. The experimental ground-state spectroscopic factor was varied with its experimental uncertainty while the three theoretical values calculated for the first excited state assumed a factor uncertainty of 2. After varying the spectroscopic factor, the corresponding astrophysical S factors $S(E_0)$ were scaled to calculate the new S factor before summing all four contributions in the direct capture component calculation. The results for the calculated rate for the 23 Al (p, γ) rate can be found in Table II.

We assessed the impact of the new ²⁴Si mass on the onset of the αp process by calculating the flow at the ²²Mg bottleneck. To first order, at this point in the reaction network, there is a competition between $^{23}\text{Al}(p, \gamma)$ and $^{22}\text{Mg}(\alpha, p)$, given the rather long half-life of ²²Mg, 3.88 s [42], and the low proton separation energy S_p of ²³Al, 0.141 MeV [13]. The flow into the αp process is defined as $\lambda_{\alpha,p}/(\lambda_{p,\gamma} + \lambda_{\alpha,p})$. The rates are $\lambda_i = W(X_i/A_i)\rho N_A \langle \sigma v \rangle$, where X_i and A_i are the mass fraction and mass number of hydrogen and helium for the ²³Al (p, γ) and ²²Mg (α, p) reactions, respectively [43]. W is a weight factor, which is the equilibrium abundance of the nuclide as determined by the Saha equation [6,44]. Since the ²²Mg β^+ -decay rate is too slow to compete, only strong and electromagnetic interactions are involved in the flow, and the density dependence cancels. For X_i , we take the conditions determined by Ref. [45] for the x-ray burst ignition region, where $X_{\rm H} = 0.03$ and $X_{\rm He} = 0.31$.

Results are shown in Fig. 3 over the range of temperatures of relevance for x-ray bursts. For the following discussion, we adopt 10% of flow through $^{22}{\rm Mg}(\alpha,p)$ as the point when the αp process becomes significant. Previously, using the $^{23}{\rm Al}(p,\gamma)$ reaction rate uncertainty from Ref. [16], the uncertainty band for when the αp process becomes significant is $T_9 = 0.94 \pm 0.15$ GK. With the new $^{24}{\rm Si}$ mass, this uncertainty band becomes 0.93 ± 0.08 GK, precisely pinpointing the onset of the αp process in x-ray bursts. While adopting other ignition conditions shifts the temperature for significant αp -process flow, e.g., 0.99 ± 0.09 GK for the $X_{\rm H} =$

TABLE II. The recommended reaction rate based on information from Ref. [16] and this work. Also included are the lower (16th percentile) and upper (64th percentile) uncertainties of this reaction.

T_9	Ν	$N_A \langle \sigma v \rangle$ (cm ³ /s/mole)			
	Recommended	Lower	Upper		
0.1	8.195×10^{-7}	4.777×10^{-7}	1.402×10^{-6}		
0.15	2.754×10^{-4}	1.640×10^{-4}	4.642×10^{-4}		
0.2	4.481×10^{-3}	2.602×10^{-3}	7.761×10^{-3}		
0.3	6.168×10^{-2}	3.432×10^{-2}	1.114×10^{-1}		
0.4	2.022×10^{-1}	1.099×10^{-1}	3.746×10^{-1}		
0.5	3.834×10^{-1}	2.052×10^{-1}	7.212×10^{-1}		
0.6	5.594×10^{-1}	2.967×10^{-1}	1.064		
0.7	7.096×10^{-1}	3.745×10^{-1}	1.360		
0.8	8.328×10^{-1}	4.392×10^{-1}	1.601		
0.9	9.381×10^{-1}	4.950×10^{-1}	1.801		
1.0	1.034	5.482×10^{-1}	1.979		
1.5	1.707	9.329×10^{-1}	3.303		
2.0	3.222	2.010	6.553		

0.06 and $X_{\rm He} = 0.19$ ignition conditions from the calculations of Ref. [43], the precision remains 9%. Therefore, we firmly establish the relevance of the αp process in powering x-ray burst light curves by determining under which conditions there is (α, p) breakout from the ²²Mg waiting point.

This Letter presents the first high-precision mass measurement of 24 Si using Penning trap mass spectrometry, resulting in a mass excess of $10\,753.8(37)$ keV. The achieved precision reduces the uncertainty of the 23 Al (p,γ) reaction rate, pinpointing the temperature when the the αp process turns on in x-ray bursts with 22 Mg (α,p) to 9%. Further refinement would require more precise resonance strength determinations for 23 Al (p,γ) , as was recently submitted for publication [46], and a measurement of the 22 Mg (α,p) cross section to lower center-of-mass energies.

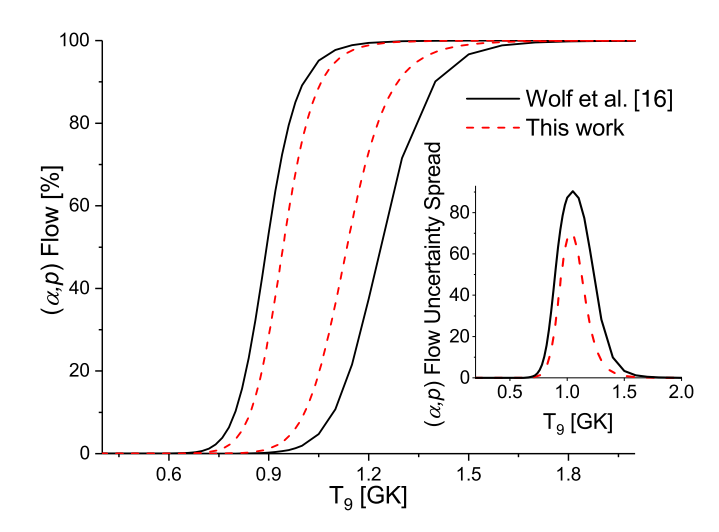


FIG. 3. Flow through $^{22}{\rm Mg}(\alpha,p)$ for the temperature range of relevance for x-ray bursts, where the solid black lines assume the $^{23}{\rm Al}(p,\gamma)$ reaction rate uncertainty of Ref. [16] and the dashed red lines correspond to the uncertainty from this work. The inset shows the uncertainty spread in the (α,p) flow, which peaks at temperatures reached during the light curve rise in x-ray burst model calculations.

This material is based upon work supported by the U.S. National Science Foundation through Grants No. PHY-1565546, No. PHY-2111185 (The Precision Frontier at FRIB: Masses, Radii, Moments, and Fundamental Interactions), No. PHY-1430152 (Joint Institute for Nuclear Astrophysics – Center for the Evolution of the Elements), and No. PHY-191355, as well as the U.S. Department of Energy, Office of Science, Office of Nuclear Physics under Grants No. DE-FG02-88ER40387, No. DE-SC0019042, No. DE-NA0003909, and DE-SC0015927. A.A.V. acknowledges support from the NSERC (Canada) under Contract No. SAPPJ2018-00028. Part of this work was performed under the auspices of the U.S. Department of Energy by Lawrence Livermore National Laboratory under Contract No. DE-AC52-07NA27344.

^[1] W. H. Lewin, J. Van Paradijs, and R. E. Taam, Space Sci. Rev. 62, 223 (1993).

^[2] H. Schatz and K. Rehm, Nucl. Phys. A 777, 601 (2006).

^[3] H. Schatz, A. Aprahamian, J. Görres, M. Wiescher, T. Rauscher, J. Rembges, F.-K. Thielemann, B. Pfeiffer, P. Möller, K.-L. Kratz, H. Herndl, B. Brown, and H. Rebel, Phys. Rep. 294, 167 (1998).

^[4] R. Wallace and S. E. Woosley, Astrophys. J., Suppl. Ser. 45, 389 (1981).

^[5] P. Bult, D. Altamirano, Z. Arzoumanian, A. V. Bilous, D. Chakrabarty, K. C. Gendreau, T. Güver, G. K. Jaisawal, E. Kuulkers, C. Malacaria, M. Ng, A. Sanna, and T. E. Strohmayer, Astrophys. J. 907, 79 (2021).

^[6] Z. Meisel, A. Deibel, L. Keek, P. Shternin, and J. Elfritz, J. Phys. G: Nucl. Part. Phys. 45, 093001 (2018).

^[7] H. Schatz, A. Aprahamian, V. Barnard, L. Bildsten, A. Cumming, M. Ouellette, T. Rauscher, F.-K. Thielemann, and M. Wiescher, Phys. Rev. Lett. 86, 3471 (2001).

^[8] A. Heger, A. Cumming, D. K. Galloway, and S. E. Woosley, Astrophys. J. Lett. 671, L141 (2007).

^[9] M. Zamfir, A. Cumming, and D. K. Galloway, Astrophys. J. 749, 69 (2012).

^[10] R. H. Cyburt, A. M. Amthor, A. Heger, E. Johnson, L. Keek, Z. Meisel, H. Schatz, and K. Smith, Astrophys. J. 830, 55 (2016).

^[11] A. Parikh, J. José, F. Moreno, and C. Iliadis, Astrophys. J., Suppl. Ser. 178, 110 (2008).

^[12] J. L. Fisker, F.-K. Thielemann, and M. Wiescher, Astrophys. J. 608, L61 (2004).

^[13] W. Huang, M. Wang, F. Kondev, G. Audi, and S. Naimi, Chin. Phys. C 45, 030002 (2021).

^[14] L. van Wormer, J. Görres, C. Iliadis, M. Wiescher, and F.-K. Thielemann, Astrophys. J. 432, 326 (1994).

^[15] J. S. Randhawa *et al.*, Phys. Rev. Lett. **125**, 202701 (2020).

^[16] C. Wolf et al., Phys. Rev. Lett. 122, 232701 (2019).

- [17] D. Morrissey, B. Sherrill, M. Steiner, A. Stolz, and I. Wiedenhoever, Nucl. Instrum. Methods Phys. Res., Sect. B 204, 90 (2003).
- [18] C. Sumithrarachchi, D. Morrissey, S. Schwarz, K. Lund, G. Bollen, R. Ringle, G. Savard, and A. Villari, Nucl. Instrum. Methods Phys. Res., Sect. B 463, 305 (2020).
- [19] R. Ringle, S. Schwarz, and G. Bollen, Int. J. Mass Spectrom. 349–350, 87 (2013).
- [20] S. Schwarz, G. Bollen, R. Ringle, J. Savory, and P. Schury, Nucl. Instrum. Methods Phys. Res., Sect. A 816, 131 (2016).
- [21] R. Ringle, G. Bollen, A. Prinke, J. Savory, P. Schury, S. Schwarz, and T. Sun, Nucl. Instrum. Methods Phys. Res., Sect. A 604, 536 (2009).
- [22] R. Ringle, G. Bollen, A. Prinke, J. Savory, P. Schury, S. Schwarz, and T. Sun, Int. J. Mass Spectrom. 263, 38 (2007).
- [23] K. Blaum, D. Beck, G. Bollen, P. Delahaye, C. Guénaut, F. Herfurth, A. Kellerbauer, H.-J. Kluge, D. Lunney, S. Schwarz, L. Schweikhard, and C. Yazidjian, Europhys. Lett. 67, 586 (2004).
- [24] A. Kwiatkowski, G. Bollen, M. Redshaw, R. Ringle, and S. Schwarz, Int. J. Mass Spectrom. 379, 9 (2015).
- [25] G. Bollen, R. B. Moore, G. Savard, and H. Stolzenberg, J. Appl. Phys. 68, 4355 (1990).
- [26] M. König, G. Bollen, H.-J. Kluge, T. Otto, and J. Szerypo, Int. J. Mass Spectrom. Ion Processes 142, 95 (1995).
- [27] M. Kretzschmar, Int. J. Mass Spectrom. 264, 122 (2007).
- [28] R. T. Birge, Phys. Rev. 40, 207 (1932).
- [29] K. Gulyuz, J. Ariche, G. Bollen, S. Bustabad, M. Eibach, C. Izzo, S. J. Novario, M. Redshaw, R. Ringle, R. Sandler, S. Schwarz, and A. A. Valverde, Phys. Rev. C 91, 055501 (2015).
- [30] L. S. Brown and G. Gabrielse, Rev. Mod. Phys. 58, 233 (1986).
- [31] R. Ringle, T. Sun, G. Bollen, D. Davies, M. Facina, J. Huikari, E. Kwan, D. J. Morrissey, A. Prinke, J. Savory, P. Schury, S. Schwarz, and C. S. Sumithrarachchi, Phys. Rev. C 75, 055503 (2007).

- [32] G. R. Burleson, G. S. Blanpied, G. H. Daw, A. J. Viescas, C. L. Morris, H. A. Thiessen, S. J. Greene, W. J. Braithwaite, W. B. Cottingame, D. B. Holtkamp, I. B. Moore, and C. F. Moore, Phys. Rev. C 22, 1180 (1980).
- [33] C. Iliadis, R. Longland, A. Champagne, A. Coc, and R. Fitzgerald, Nucl. Phys. A **841**, 31 (2010).
- [34] W. A. Fowler, G. R. Caughlan, and B. A. Zimmerman, Annu. Rev. Astron. Astrophys. 5, 525 (1967).
- [35] B. A. Brown and W. D. M. Rae, Nucl. Data Sheets 120, 115 (2014).
- [36] B. Longfellow, A. Gade, J. A. Tostevin, E. C. Simpson, B. A. Brown, A. Magilligan, D. Bazin, P. C. Bender, M. Bowry, B. Elman, E. Lunderberg, D. Rhodes, M. Spieker, D. Weisshaar, and S. J. Williams, Phys. Rev. C 101, 031303(R) (2020).
- [37] J. Humblet, W. A. Fowler, and B. A. Zimmerman, Astron. Astrophys. 177, 317 (1987).
- [38] J. Henderson and S. R. Stroberg, Phys. Rev. C **102**, 031303(R) (2020).
- [39] R. Longland, C. Iliadis, A. Champagne, J. Newton, C. Ugalde, A. Coc, and R. Fitzgerald, Nucl. Phys. A 841, 1 (2010).
- [40] W. A. Richter, B. A. Brown, R. Longland, C. Wrede, P. Denissenkov, C. Fry, F. Herwig, D. Kurtulgil, M. Pignatari, and R. Reifarth, Phys. Rev. C 102, 025801 (2020).
- [41] A. Banu, F. Carstoiu, N. L. Achouri, W. N. Catford, M. Chartier, B. Fernández-Domínguez, M. Horoi, B. Laurent, N. A. Orr, S. Paschalis, N. Patterson, B. Pietras, B. T. Roeder, P. Roussel-Chomaz, J. S. Thomas, L. Trache, and R. E. Tribble, Phys. Rev. C 86, 015806 (2012).
- [42] M. S. Basunia, Nucl. Data Sheets 127, 69 (2015).
- [43] G. Merz and Z. Meisel, Mon. Not. R. Astron. Soc. 500, 2958 (2020).
- [44] E. Brown, *Stellar Astrophysics* (Open Astrophysics Bookshelf, 2015)
- [45] J. L. Fisker, H. Schatz, and F.-K. Thielemann, Astrophys. J., Suppl. Ser. 174, 261 (2008).
- [46] G. Lotay (private communication).